Quantum Fluids of Light*

Emmanuel Mercado Gutierrez†
(Dated: November 20, 2018)

In this work we are going to introduce the concepts about quantum fluids of light , starting from what are the characteristics of the system in which fluids of light are studied and know a set o new quasiparticles as exciton and polaritons. Also, we are going to show how are trapped this particles in a microcavity, generating a confining potential for photons and quasi-particles. We are going to show two experiments in which are reached Bose-Einstein condensate of light showing the characteristic of their superfluid properties

Keywords: keys.

I. INTRODUCTION

One of the most striking quantum effects in an interacting Bose gas at low temperature is superfluidity. First observed in liquid ^{4}He[1, 6], this phenomenon has been intensively studied in a variety of systems for its remarkable features such as the persistence of superflows and the proliferation of quantized vortices. The achievement of Bose–Einstein condensation in dilute atomic gases provided the opportunity to observe and study superfluidity in an extremely clean and wellcontrolled environment[2, 5]. In the solid state, Bose–Einstein condensation of exciton polaritons now allows to plan for the observation of similar phenomenology[3, 7]. Polaritons are interacting light–matter quasiparticles that occur naturally in semiconductor microcavities in the strong coupling regime and constitute an interesting example of composite bosons. Historically, the area of quantum fluids of light research (theoretical and experimental) deals with massive material particules (atoms, electrons). However, we know since the early days of quantum mechanics, that photons in a box can be interpreted as a massless Bose gas of non-interacting particules. This fruitful interpretation leads for example to the correct black-body radiation spectrum. Recently, it has been realized that under suitable circumstances photons can acquire an effective mass and will behave as a quantum fluid of light with photon-photon interactions.

II. FUNDAMENTAL CONCEPTS

An optical cavity is an arrangement of mirrors that form a standing wave for light waves. Light confined in the cavity reflects multiple times producing standing waves for certain resonant frequencies. The standing wave patterns produced are called modes; longitudinal modes differ only in frequency while transverse modes differ for different frequencies and have different intensity patterns across the cross section of the beam. The most common type of optical cavities consist of two mirrors that can be flat, named of planar cavities, or curved, which are for example spherical cavities as show in figure 1. Depending of the mirrors geometry its possible to obtain a cavity with different properties, allowing the control on the cavity modes or even provide a high quality factor for the cavity.

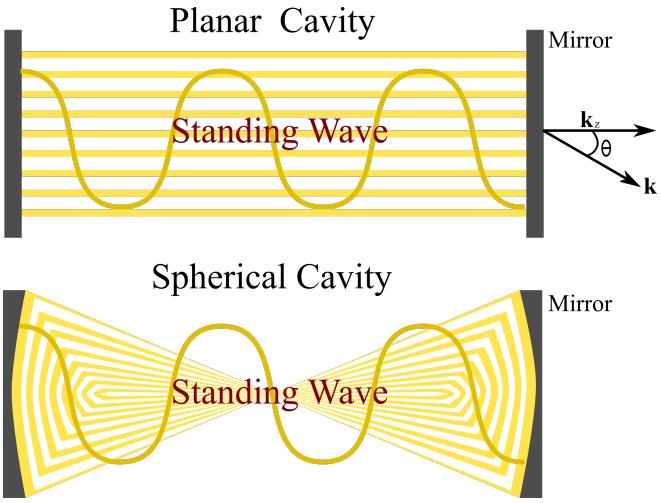

Figure 1. Examples of planar optical cavity and spherical optical cavity.

A. The two-dimensional photon field

The planar cavity is invariant under plane translation, but is better to use the wave vector $\mathbf{k}$ of the photons inside the cavity. So, vector propagation $\mathbf{k}$ form an angle θ respect to the normal vector of the planar cavity.

The free photons into the cavity can be described by the Hamiltonian.

$$H_{cav} = \int \frac{d^2\mathbf{k}}{(2\pi)^2} \sum_{\sigma} \hbar\omega_{cav}(\mathbf{k}) a^{\dagger}_{C,\sigma}(\mathbf{k})\, a_{C,\sigma}(\mathbf{k}), \qquad (1)$$

where $a_{C,\sigma}(\mathbf{k})$ and $a^{\dagger}_{C,\sigma}(\mathbf{k})$ destroy and create a cavity photon C with polarization σ and in-plane wave vector $\mathbf{k}$.

* Rev. Mod. Phys., Vol. 85, No. 1, January–March 2013
† Instituto de Física de São Carlos, Universidade de São Paulo, C.P. 369, 13560-970 São Carlos, SP, Brazil.

$\omega_{cav}(\mathbf{k})$ is the frequency for photons with mode $\mathbf{k}$. Photons are Bosons that satisfy the commutation relations rules:

$$\left[a_{C,\sigma}(\mathbf{k}), a^{\dagger}_{C,\sigma'}(\mathbf{k}')\right] = (2\pi)^2 \delta(\mathbf{k}-\mathbf{k}') \quad (2)$$

$$\delta_{\sigma,\sigma'}\left[a_{C,\sigma}(\mathbf{k}), a_{C,\sigma'}(\mathbf{k}')\right] = 0 \quad (3)$$

Two -dimensional cavity photons field operator $\Psi_{C,\sigma}$ and $\Psi^{\dagger}_{C,\sigma}$ are defined through the Fourier transform of creation and annihilation operators,

$$\Psi_{C,\sigma}(\mathbf{r}) = \int \frac{d^2\mathbf{k}}{(2\pi)^2} a_{C,\sigma}(\mathbf{k}) e^{i\mathbf{k}\cdot\mathbf{r}},$$

which also satisfy the Bose commutation rules.

The physical observable into the cavity is the electric field, that could be expressed in term of the field operators by

$$E(\mathbf{r},z) = \int \frac{d^2\mathbf{k}}{(2\pi)^2} \sum_{\sigma} e^{i\mathbf{k}\cdot\mathbf{r}} E_{\sigma}(\mathbf{k},z)\, a_{C,\sigma}(\mathbf{k}) + h.c$$

where the z dependence of the electric field depends of the nature of the cavity mirrors. When they are separated by a distance l_z and are planar, which is the case, the profile of the electric field along the z directions has the typical profile for the lowest mode as follows,

$$E_{\sigma}(\mathbf{k},z) = \sqrt{\frac{4\pi\hbar\omega_{cav}}{l_z n_0^2}} \sin\left(\frac{\pi z}{l_z}\right)\hat{e}_{\sigma},$$

where, n_0 is the refractive index of the planar cavity and $\hat{e}_{\sigma}$ is the unit vectors in the polarization basis. The effects of the polarization light when we consider modes from $k \ll 1$ (small k limit) and different from zero, becomes into the splitting of the transverse electric (TE) and transverse magnetic (TM) linear polarization states, which can be understood as for example the spin-orbit interaction, in which the orbital term is the wave vector $\mathbf{k}$ and the «spin» term correspond to polarization in the basis $\sigma^{\pm}$. If we go further, into the description of the physics of free photons in a cavity, we are going to find two extra terms in the Hamiltonian (1), that correspond to the pumping and losses terms, leaving the discussion to the input-output theory of optical cavities, which is out of the scope of this work. Now we are focus on the production of the interactions between photons and the origin of the new set of quasi-particles as *excitons* and *polaritons*.

B. Optical nonlinearities and effective photon-photon interactions

In the previous section the physics was conduced by the linear effects in the optical cavity but, when the cavity is immersed in a sizable nonlinear material new phenomena appears, as a consequence of the wave mixing processes that coupling the modes of the cavity with the material media.

For a large number of photons in the nonlinear media, the interactions of photons due to the material can be described by the form:

$$H_{cav-cav} = \frac{1}{2}\frac{1}{(2\pi)^3}\int d^2\mathbf{k}d^2\mathbf{k}'d^2\mathbf{q} \sum_{\sigma,\sigma'} V^{cav-cav}_{\sigma,\sigma'}(\mathbf{k},\mathbf{k}'\mathbf{q}) \times a^{\dagger}_{C,\sigma}(\mathbf{k}+\mathbf{q})\, a^{\dagger}_{C,\sigma'}(\mathbf{k}'-\mathbf{q}) a_{C,\sigma'}(\mathbf{k}')\, a_{C,\sigma}(\mathbf{k}) \quad (4)$$

where $V^{cav-cav}_{\sigma,\sigma'}(\mathbf{k},\mathbf{k}'\mathbf{q})$ is the photon-photon interaction potential and the polarization σ and σ' are in the circular polarization basis, where the total momentum is conserved. As the typical length scale of the electron dynamics in typical bulk material media and in semiconductor heterostructures used for quantum fluid effects is much shorter than the optical wavelength along the plane, the interaction potential $V^{cav-cav}_{\sigma,\sigma'}$;0 can be approximated with its zero-momentum value $V^{0}_{\sigma,\sigma'}$ $\mathbf{k}=\mathbf{k}'=\mathbf{q}$ =0: In real space, this corresponds to assuming that photon-photon interaction occur via a local potential,

$$H_{cav-cav} = \int d^2\mathbf{r} \frac{V^{0}_{\sigma,\sigma'}}{2} \Psi^{\dagger}_{C,\sigma}(\mathbf{r})\, \Psi^{\dagger}_{C,\sigma'}(\mathbf{r})\, \Psi_{C,\sigma'}(\mathbf{r})\, \Psi_{C,\sigma}(\mathbf{r})$$

As we shall see, this photon-photon interaction is mediated by the excitation of pair particle-hole of the nonlinear material. In the simplest case when the photon frequencies that are involved in the photon fluid dynamics are very far away from electronic resonances in the nonlinear optical material, the optical transitions are virtual and the populations of the excited electronic states remains negligible. On the other hand the strong limit regime is achieved when the mode of the cavity is strongly coupled to narrow transition in the optical medium, in this case, the photon inherits the strong nonlinearity of the matter excitation. To talk a little bit about the composition of the nonlinear media, we are going to consider that a thin layer of a semiconductor that are parallel with the cavity plane, in which are embedded one or more quantum well (QW). The chemical composition of the well is chose to have the botton of the conduction band at a lower energy and the top of the valence band at a higher energy than the surrounding material, thus producing quantum confinement of both electrons and holes. The excitation in the optical material is composed for a hole that has positive charge, and an electron interacting through coulomb potential. This pair particle-hole is treated as a quasiparticle named *exciton*.

In order to undertand how is the formation of an exciton, we are going to consider a photon incoming into the semiconductor exciting an electron from valence band

to conduction band , creating a bounded pair particle-hole. This new quasiparticle is hydrogenlike in which the bound energy is less that the hydrogen atom bound energy. To maximize the strong coupling of their electronic degrees of freedom, the layer with the quantum well is placed in the antinodes of the cavity field, and the cavity field ω_{cav}^{0} is tuned in the vicinity of the QW *exciton* frequency ω_{exc}. The *exciton* frequency is weakly dependent on the in-plane wave vector $\mathbf{k}$, where $\omega_{exc}(\mathbf{k}) \approx \omega_{exc}^{0} + \hbar k^2/2m_{exc}$. The behavior of the *exciton* is like bosonic particles that can be expressed in function of the creation and annihilation operators, $a(\mathbf{k})_{X,\sigma}$ and $a(\mathbf{k})_{X,\sigma}^{\dagger}$, respectively.

The dynamic and the coupling with the cavity field can be expressed with the Hamiltonian,

$$H_{exc} = \int \frac{d^2\mathbf{k}}{(2\pi)^2} \sum_{\sigma} \hbar\{\omega_{exc}(\mathbf{k})\, a(\mathbf{k})_{X,\sigma}^{\dagger}\, a(\mathbf{k})_{X,\sigma} + \Omega_R \left[a(\mathbf{k})_{X,\sigma}^{\dagger}\, a(\mathbf{k})_{C,\sigma} + a(\mathbf{k})_{C,\sigma}^{\dagger}\, a(\mathbf{k})_{X,\sigma}\right]\} \quad (5)$$

where the first term of the hamiltonian represent the dynamics of the free *excitons* and the second term, the coupling with photon cavities, when a cavity photon is "absorbed" (destroyed) an *exciton* is created and vice-versa. All of this with amplitude of the Rabi frequency Ω_r that couple the quantum well excitation and the cavity photon electric field.

The total Hamiltonian of the system until now a combination of the free photon cavity and the *exciton* dynamics which result into an effective Hamiltonian,

$$H_{cav} + H_{exc} = \int \frac{d^2\mathbf{k}}{(2\pi)^2} \sum_{\sigma} (\hbar\omega_{cav}(\mathbf{k}) a_{C,\sigma}^{\dagger}(\mathbf{k})\, a_{C,\sigma}(\mathbf{k}) + \hbar\{\omega_{exc}(\mathbf{k})\, a(\mathbf{k})_{X,\sigma}^{\dagger}\, a(\mathbf{k})_{X,\sigma} + \Omega_R a(\mathbf{k})_{X,\sigma}^{\dagger}\, a(\mathbf{k})_{C,\sigma} + \Omega_R a(\mathbf{k})_{C,\sigma}^{\dagger}\, a(\mathbf{k})_{X,\sigma}\}) \quad (6)$$

which can be expressed in a diagonal form through the bogoulivov transformations,

$$a_{C,\sigma}(\mathbf{k}) = u_c^{LP}(\mathbf{k})\, a_{LP,\sigma}(\mathbf{k}) + u_c^{UP}(\mathbf{k})\, a_{UP,\sigma}(\mathbf{k})$$
$$a_{X,\sigma}(\mathbf{k}) = u_x^{LP}(\mathbf{k})\, a_{LP,\sigma}(\mathbf{k}) + u_x^{UP}(\mathbf{k})\, a_{UP,\sigma}(\mathbf{k}),$$

where u_c and u_x are the Hopfield coefficients that represents the excitonic and photonic weights in the new system. If we replacing this into the hamiltonian 6 we can obtain:

$$H_0 = \int \frac{d^2\mathbf{k}}{(2\pi)^2} \{a_{LP,\sigma}^{\dagger}(\mathbf{k})\, a_{LP,\sigma}(\mathbf{k}) \left(\hbar\omega_{cav} \left|u_c^{LP}\right|^2 + \hbar\omega_{exc} \left|u_x^{LP}\right|^2 + \Omega_R \left[\left(u_x^{LP}\right)^* u_c^{LP} + \left(u_c^{LP}\right)^* u_x^{LP}\right]\right) + a_{UP,\sigma}^{\dagger}(\mathbf{k})\, a_{UP,\sigma}(\mathbf{k}) \left(\hbar\omega_{cav} \left|u_c^{UP}\right|^2 + \hbar\omega_{exc} \left|u_x^{UP}\right|^2 + \Omega_R \left[\left(u_x^{UP}\right)^* u_c^{UP} + \left(u_c^{LP}\right)^* u_x^{LP}\right]\right) + NLT \quad (7)$$

where NLT means nonlienar terms that depends on $a_{(LP,UP),\sigma}(\mathbf{k})\, a_{LP,\sigma}(\mathbf{k})$ and $a_{LP,\sigma}^{\dagger}(\mathbf{k})\, a_{LP,\sigma}^{\dagger}(\mathbf{k})$This Hamiltonian is diagonal in the new basis $a_{LP}(\mathbf{k})$ and $a_{UP}(\mathbf{k})$ taking the coefficients for the nonliear part equal to zero. This leads to the simplified Hamiltonian,

$$H_0 = \int \frac{d^2\mathbf{k}}{(2\pi)^2} \sum_{\sigma} [\hbar\omega_{LP,\sigma}(\mathbf{k})\, a_{LP,\sigma}^{\dagger}(\mathbf{k})\, a_{LP,\sigma}(\mathbf{k}) + \hbar\omega_{UP,\sigma}(\mathbf{k})\, a_{UP,\sigma}^{\dagger}(\mathbf{k})\, a_{UP,\sigma}(\mathbf{k})] \quad (8)$$

where $a_{LP,\sigma}(\mathbf{k})$ and $a_{UP,\sigma}(\mathbf{k})$ are operators that make diagonal the Hamiltonian resulting from the linear superposition of exciton and cavity modes, the so-called *exciton polaritons*. LP and UP refers to lower and upper polariton, and the dispersion ω_{LP} and ω_{UP} are given by

$$\omega_{(UP,\,LP)}(\mathbf{k}) = \frac{\omega_{cav,\sigma}(\mathbf{k}) + \omega_{exc,\sigma}(\mathbf{k})}{2} \pm \left[\Omega_R^2 + \left(\frac{\omega_{cav,\sigma}(\mathbf{k}) - \omega_{exc}(\mathbf{k})}{2}\right)^2\right]^{1/2} \quad (9)$$

in which, the plus-minus terms correspond to the upper polariton and lower polariton branch respectively and the minimum difference between the two branches is dependent of Ω_R. In the figure 2 we can see the the plot of the dispersion energy for two branch as a function of wave vector in z direction $\mathbf{k}_z$ in a CdTe-based microcavity. We can observe that for the strong coupling limit, which mean in the limit for small $\mathbf{k}$, both branches has a minimum of energy. Close to the crossing point, both polariton modes have approximately equal photon and exciton content , $\left|u_{x,c}^{LP}\right|^2 = \left|u_{x,c}^{UP}\right|^2 \approx 1/2$, while farther away the two polariton branches acquire a purely excitonic or photonic character.

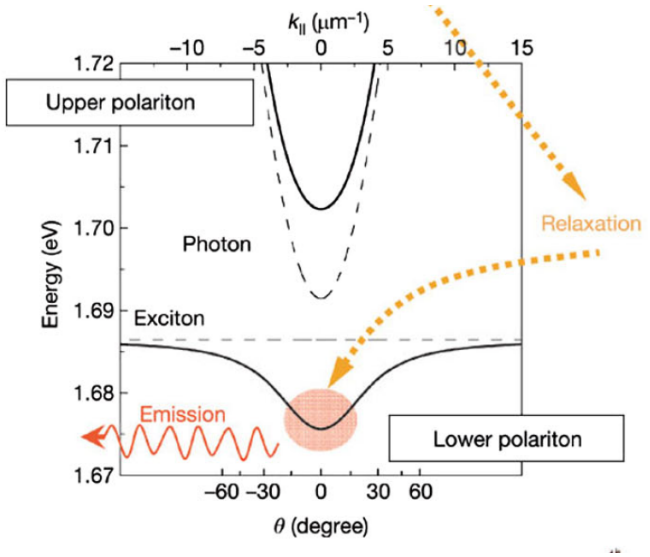

Figure 2. Energy spectrum of polariton as a function of the in-plane wavevector $\mathbf{k}_z$ in a CdTe-based microcavity. Interaction between exciton and photon modes, with parabolic dispersions (dashed curves), gives rise to lower and upper polariton branches (solid curves) with dispersions featuring an anticrossing typical of the strong coupling regime. The excitation laser is at high energy and excites free carrier states of the quantum well. Relaxation towards the exciton level and the bottom of the lower polariton branch occurs by acoustic and optical phonon interaction and polariton scattering. The radiative recombination of polaritons results in the emission of photons that can be used to probe their properties. Photons emitted at angle v correspond to polaritons of energy E and in-plane wavevector $\mathbf{k}_z = (E/\hbar c)\sin\theta$[7].

C. External potentials affecting the in-plane motion of cavity excitation

The effective external potential that cavity photons and excitons can see, can be expressed using the Hamiltonian

$$H_{pot} = \int d^2\mathbf{r} \sum_{\sigma,\sigma'} [V^{cav}_{\sigma,\sigma'}(\mathbf{r})\,\Psi^{\dagger}_{cav,\sigma}(\mathbf{r})\,\Psi_{cav,\sigma'}(\mathbf{r}) + V^{exc}_{\sigma,\sigma'}(\mathbf{r})\,\Psi^{\dagger}_{exc,\sigma}(\mathbf{r})\,\Psi_{exc,\sigma'}(\mathbf{r}) \quad (10)$$

provided the amplitudes of the potentials V^{cav} and V^{exc} are much smaller that the rabi energy $\hbar\Omega_R$ and for a sufficiently smooth spatial variation, the resulting potential acting on lower polaritons can be written as

$$V^{LP}_{\sigma,\sigma'}(\mathbf{r}) = \left|u^{LP}_c\right|^2 V^{cav}_{\sigma,\sigma'}(\mathbf{r}) + \left|u^{LP}_x\right|^2 V^{exc}_{\sigma,\sigma'}(\mathbf{r}) \quad (11)$$

In analogy with atomic gases, the potential can be attractive or repulsive, even spin dependent, in order to confine or spell the quasiparticles. We are going to see in the next section that its possible to create a attractive potential for excitons applying a mechanical stress in the nonlinear material sample [4]. Another way to create and effective potential is, cavity layer with thickness dependence, feature that allow obtain a full scan of the exciton-photon detuning across the resonance on a single microcavioty sample. Another way of confining polaritons is to design a micropillar structure by etching away all the layers forming the top mirror and the cavity layer (and possibly also the lower mirror down to the substrate): In this case, light is confined in the in-plane directions by the large refractive index mismatch at the air-semiconductor interface.

D. Polariton-Polariton Interaction

Once the polaritons feel the spatial potential they can interact each other. As it is typically done in the many-body physics, a common procedure is to describe the system in terms of an effective model Hamiltonian that is able to reproduce the interactions between excitons without invoking their elementary constituents, this mean that we are going to replace the coulomb interaction by a simple two-body interaction potential for exciton, this can be expressed in terms of the Hamiltonina

$$H_{XX} = \int \mathrm{d}^2\mathrm{r} \sum_{\sigma\sigma'} \frac{V^{XX}_{\sigma,\sigma'}}{2} \Psi^{\dagger}_{X,\sigma}(\mathbf{r})\,\Psi^{\dagger}_{X,\sigma'}(\mathbf{r})\,\Psi_{X,\sigma'}(\mathbf{r})\,\Psi_{X,\sigma}(\mathbf{r}) \quad (12)$$

where the spin indices σ, σ' run over the circular polarization basis. Rotational invariance for a contact interaction potential imposes that total exciton spin is conserved[] and that $V^{XX}_{\sigma^+,\sigma^+} = V^{XX}_{\sigma^-,\sigma^-} = V^{XX}_T$ and $V^{XX}_{\sigma^+,\sigma^-} = V^{XX}_{\sigma^-,\sigma^+} = V^{XX}_S$. An estimation of the value of V^{XX} was made for in which $V^{XX}_T = 6e^2 a_B/\epsilon$ where ϵ is the dielectric constant of the material and a_B is the Bohr radius. This term is most important contribution when the microcavity is excited by circularly polarized light. In principle, exciton-exciton interaction can transform a pair of $\sigma_\pm$ bright exciton into a pair of ± 2 dark excitons. While these processes are important in isolated quantum wells, they no longer conserve energy in microcavities: Because of the Rabi coupling between photons and bright excitons, the dark spin ± 2 excitons are at much higher energy than the lower polariton branch and can only play a role as nonresonant intermediate states of high-order processes. An additional interaction channel have to be considered when we consider the Pauli exclusion principle for electrons and holes where is prohibited that another exciton can be created at a distance shorter than Bohr radius from an existing exciton with the same spin. In this case and considering only the bright exciton states, this can be modeled as an effective quartic Hamiltonian term in the form

$$H_{sat} = \int \mathrm{d}^2\mathrm{r} \sum_{\sigma\sigma'} \frac{V^{sat}_{\sigma,\sigma'}}{2} \Psi^{\dagger}_{X,\sigma}(\mathbf{r}) \Psi^{\dagger}_{X,\sigma'}(\mathbf{r}) \Psi_{X,\sigma'}(\mathbf{r}) \Psi_{X,\sigma}(\mathbf{r}), \tag{13}$$

with a saturation potential $V^{sat}_{\sigma,\sigma'} = \delta_{\sigma,\sigma'}\hbar\Omega_R/n_{sat}$. The exact value of the saturation density is $n_{sat} = 1/a_B^2$ with depends on the specific shape of the internal wave function of the exciton. Depending on the cavity the saturation potential is smaller than the exciton-exciton contribution.

In relevant experimental condition only its important to consider the bottom of the lower branch, in which the approximation is parabolic. The hamiltonian 13 and 12 can be rewritten in terms on the polaritons operators considering only the lower branch as follows,

$$H_{LP-LP} = \int \mathrm{d}^2\mathrm{r} \sum_{\sigma\sigma'} \frac{V^{LP-LP}_{\sigma,\sigma'}}{2} \Psi^{\dagger}_{LP,\sigma}(\mathbf{r}) \Psi^{\dagger}_{LP,\sigma'}(\mathbf{r}) {}_{LP,\sigma'} \times \Psi_{LP,\sigma'}(\mathbf{r}) \Psi_{LP,\sigma}(\mathbf{r})$$

with

$$V^{LP-LP}_{\sigma,\sigma'} = \left|u^{LP}_x\right|^4 V^{XX}_{\sigma,\sigma'} + 2\left|u^{LP}_x\right|^2 u^{LP}_x u^{LP}_c V^{sat}_{\sigma,\sigma'}.$$

In the next section we shall see the experimental realization of exciton-polaritons and photons, and understant how the external potential are created and how the light interact we the quase-particles to reach Bose-Einstein condensation.

III. EXPERIMENTS

In order to show the experimental results of the photon fluids we are to show two different experiments, the first one is about Bose-Einstein Condensate of Microcavity polaritons in a Trap, and Bose Einstein condensation of photons in a microcavity both development by the group or Martin Weitz.

A. Bose-Einstein Condensate of Microcavity Polaritons in a Trap

In this experiment is reported the demonstration of a spatial trap for polaritons in the plane of their motion. The geometry of the confinement it approximately parabolic at its minimum. polaritons are generated with a focused laser far away from the center of the trap in such way that polaritons can accumulated in the bottom potential. Polaritons and embebed into a GaAs-based microcavity which behavior is like a weakly intereacting bose gas with extremely light mass, which implies very high critical temperature for Bose coherent effects.

As we know, Cavity photons by themselves are essentially noninteracting, but polaritons interact with each other via short-range interaction due to their exciton component. The laser beam has a incident angle of $\theta = 17^o$ and the sample was held in helium vapor at temperature $T = 4.2\,K$. Polaritons decay into photons that go out of the cavity which go out the cavity. The in-plane component of the momentum must be conserved in the conversion of polaritons to external photons, which implies that the angle of emission of a detected photon talk about the in-plane momentum of the polariton at the moment of decay. By recording the spectrum of the emitted light as a function of emission angle, it has a complete measurement of the momentum and energy distribution of the polaritons.

The potential of trap can be created in diffeten ways, one of then as we mentioned before is appliying mechanical estress in the sample with a pin, as we can see on the top of the right side in figure 3.

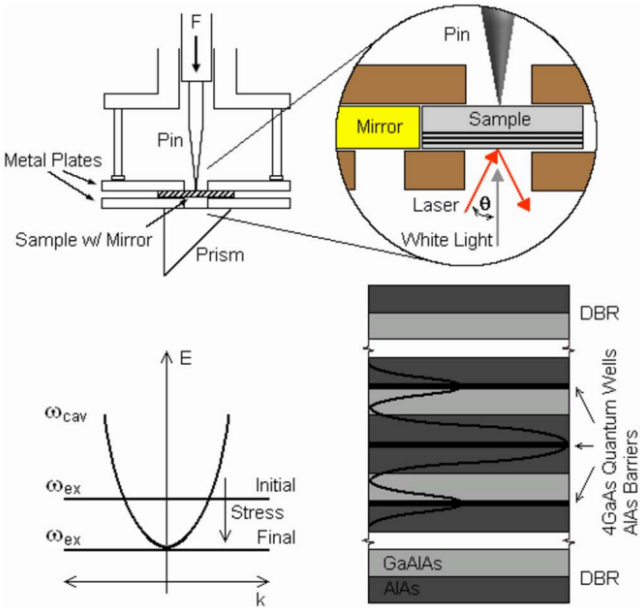

Figure 3. Color online Upper diagram: Geometry of the experiment. Lower right: The structure of the microcavity. Lower left: The effect of stress tuning.

A force is applied on the backside of the 150-μm-thick substrate with a rounded-tip pin, with approximately 50 μm tip radius. with this, the stress shifts the exciton states while the cavity photon energy is left essentially unchanged. Directly under the stressor, the lower polariton branch has an energy minimum, as is shown in figure 4. The shift of the exciton states with stress also affects the coupling of the exciton states and cavity photon states. In the center of the trap, the cavity photon states and the exciton states are strongly coupled; however, far from the center, the lowest polariton states are almost purely photon-like. This means that the trap also causes evaporative cooling, because the lifetime of the

polaritons at high energy (far from the center) is shorter than the lifetime of those at the energy minimum (in the center). Of course, this effect will work only if the polaritons have diffusion lengths long enough to move through the whole trap, where in this the experiment, in some cases polaritons can move more than 50 μm.

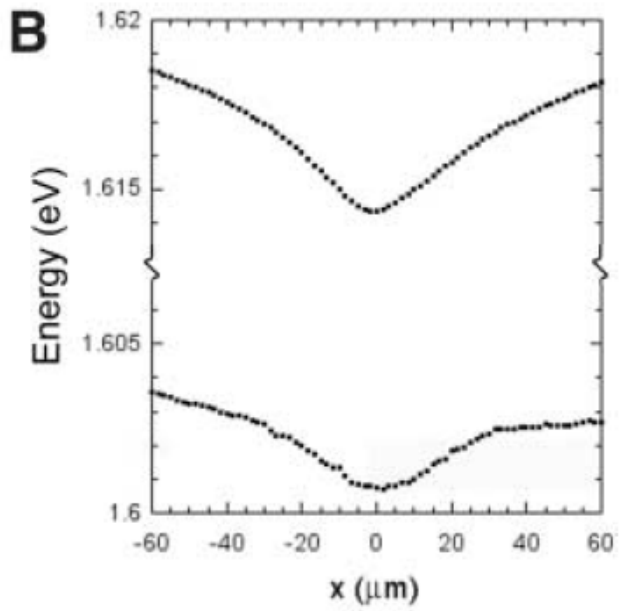

Figure 4. Difference of the external potential created by the pin when it is acting on the quantum wells.

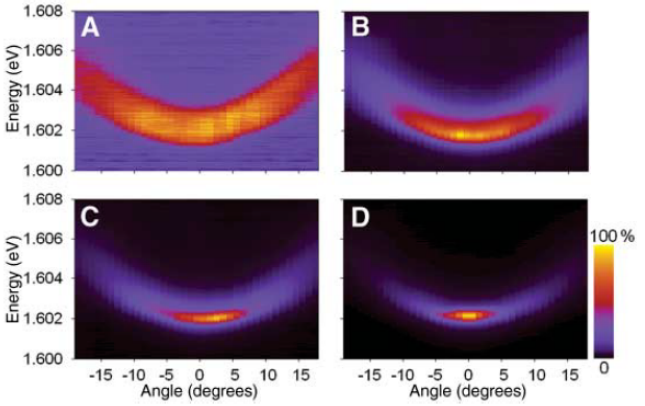

Figure 5. Momentum distribution of the polaritons as measured by angle-resolved photoluminescence intensity for four different powers. Angle-resolved spectra for (A) 0.05-mW pump power (far below the threshold density), (B) 0.4-mW pump power (just below the threshold), (C) 0.6-mW pump power (at the threshold), and (D) 0.8-mW pump power (above the threshold). The falsecolor scale is linear, with yellow and black indicating high and low values, respectively.

One of the signature of Bose-Einstein condensates is moment distribution of the particules, which can be measured for polaritons by resolvin the angular distribution of photoemission as showed in figure 5, for four different powers of the laser that creates excitons. The yellow and black color represent high and low polariton density respectively. Its possible to see the contraction of the momentum distribution, increasing the density accumulating polarons at the bottom of the lower branch. The Bose-Einstein condensation appears when more polariton are in the same phase in resonant with the cavity in the minimum of the potential.

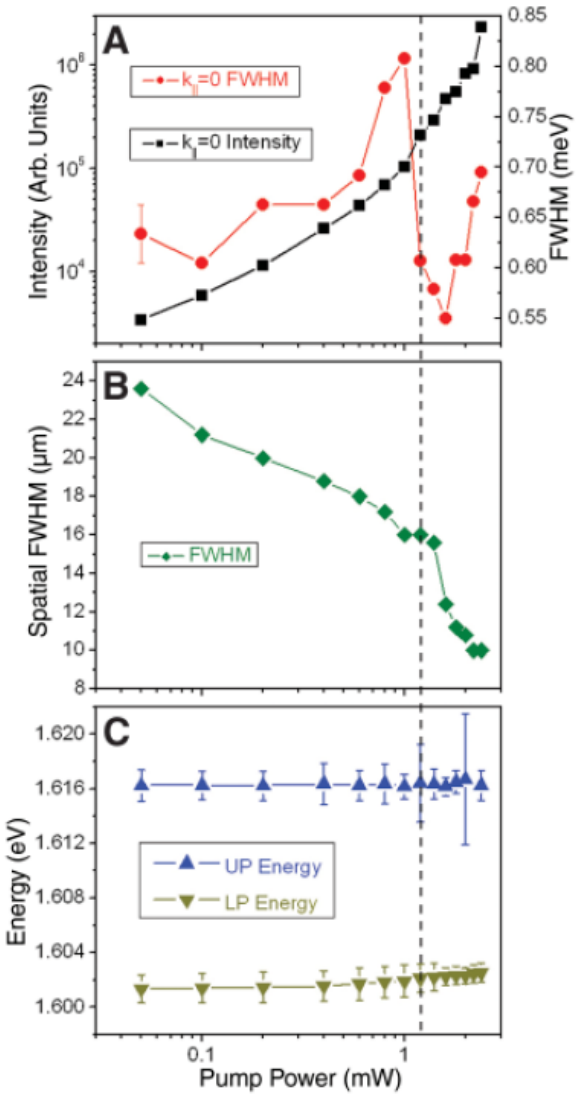

Figure 6. The black squares in A indicates total photoluminescence intensity in the longitudinal direction of the in-plane wave vector $k_z = 0$. Red circles indicate full width at half maximum (FWHM) of the emission spectrum at $k_z = 0$. In B part we have FWHM of the spatial profile of the photoluminescence collected for external angle of the excitation laser of $\theta = 0 \pm 5^{\circ}$ from the center of the trap. and in C we have that the energy of the upper and lower polariton branch do not change for different excitation power, meaning that the system remains in the strong coupling regime.

Signatures of the condensation of exciton-polaritons are illustrated in figure 6. The system is pumped with an external laser in order to conserve the total number of polaritons in the system. Polaritons in the vicinity of trap emit fluorescence linearly with the total number of the system, but the spectral emission of the emitted light is wide due to the incoherent contribution of each polariton. When the system reach a critical number of polaritons at certain critical power of excitation, the large of the spectral emission drops sharply while the fluorescence is rising, indicating that a consider number of polariton make a phase transition in which all of them are in a coherent phase.

Spatial contraction is also a telltale sign for condensation in a trap because the condensate seeks the ground state of the system, which (in the case of a trapped gas) is a compact state at the bottom of the trap. Below the critical density, in the normal state, the size of the cloud is determined by a steady-state balance of the pumping by the exciting laser and thermal diffusion; above the critical density, the size of the cloud is given by the size of the ground state of the manyparticle system. If interactions are neglected, the standard solution of a harmonic oscillator gives a ground-state wave function with extent $a = \sqrt{\hbar/m\omega_0}$. In the presence of particle-particle repulsion, the size of the ground state will expand (16), but its size is still expected to be small as compared to the size of the cloud of thermal particles. This is a major difference between experiments with and without traps: In a translationally invariant geometry, a superfluid will flow outward; whereas, in a trap, it will flow inward. Over the whole range of polariton density, the system remains in the strong coupling regime, as evidenced by the relatively small measured shifts of the lower and upper polariton lines

B. Bose–Einstein condensation of photons in an optical microcavity

In the previous section we saw the Bose-Einstein condensation of polaritons that is a quasi-particle conformed for the coupling between and an exciton and a photon cavity. The condensation is mainly formed when the "material part" of the polariton go to the bottom of the lower branch. Now in this article we are to show the formation of the BEC of photons reached by the group of Martin Weitz.

One of the amazing characteristics of photons is that have a vanishing chemical potentia, meaning that their number is not conserved when the temperature of the photon gas is varied, at low temperatures, photons disappear in the cavity walls instead of occupying the cavity ground state.

The experiment confines photons in a curved mirror optical micro-cavity resonator filled with a dye solution, in which photons are repeatedly absorbed and re-emitted by the dye molecules, that are equivalent a "withe wall" in comparison with a photon into a black-body system. The small distance of 3.5 optical wavelengths between the mirrors causes a large frequency spacing between adjacent longitudinal modes (the free spectral range is 7×10^{13} Hz), comparable with the spectral width of the dye, and modifies spontaneous emission. The photon dispersion inside the cavity has a quadratic dependence with a cut-off frequency of $2\pi \times 10^{14}$Hz, Thermal equilibrium of the photon gas is achieved by absorption and re-emission processes in the dye solution, which acts as heat bath and equilibrates the transverse modal degrees of freedom of the photon gas to the (rovibrational) temperature of the dye molecules . The photon frequencies will accumulate within a range $k_BT/\hbar\,(2\pi \times 6.3 \times 10^{12})$ at room temperature, above the low-frequency cut-off.

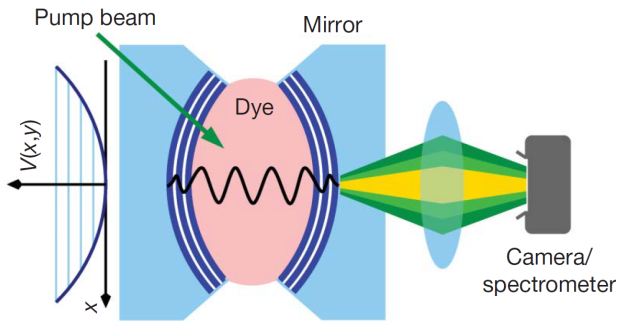

Figure 7. BEC of photons setup.

The curvature of the mirrors induce a harmonic trapping potential for photons with trap frequency of $\Omega = c/\sqrt{D_0R/2}$ with D_0 the mirror separation and R the radius of curvature. The system is formally equivalent to an ideal gas of massive bosons having an effective mass $m_{ph} = \hbar\omega_{cut-off}/c^2$.

The system is formally equivalent an ideal gas o massive boson, in which the photons have an effective mass of $m_{ph} \approx \hbar\omega_{cut-off}/c^2 \approx 6.7 \times 10^{-36}$kg. that are moving in the transverse mode of the cavity, harmonically confined with frequency $\omega_{cav} = c/\sqrt{D_0R/2} \approx 4.1 \times 10^{10}$Hz. A harmonically trapped twodimensional ideal gas exhibits BEC at finite temperature, in contrast to the two-dimensional homogeneous case.Wetherefore expect a BEC when the photon wave packets spatially overlap at low temperatures or high densities, that is, the phase space density $n\lambda_{th}^2$ exceeds a value near of unity. n is the photon density and $\lambda_{th} = h/\sqrt{2\pi m_{ph} k_B T} \approx 1.5\,\mu$m is the de Broglie wavelenght associated with the thermal motion in the cavity plane. The system reach the superfluid state when the critical number of particles is given by:

$$N_c = \frac{\pi^2}{3}\left(\frac{k_BT}{\hbar\Omega}\right)^2,$$

at room temperature the critical number is around $N_c \approx$

77000 photons.

By pumping the dye with an external laser we add to a reservoir of electronic excitations that exchanges particles with the photon gas, in the sense of a grand-canonical ensemble. The pumping is maintained throughout the measurement to compensate for losses due to coupling into unconfined optical modes, finite quantum efficiency and mirror losses.

Spatial images of the photon gas below and slightly above criticality are shown in figure 8b. In either case the lower energetic (yellow) photons are bound to the trap centre while the higher energetic (green) photons appear at the outer trap regions. Above the critical photon number a bright spot is visible in the trap centre with a full width at halfmaximum (FWHM) diameter of $(14 \pm 3)\,\mu$m, indicating a macroscopically populated TEM00-mode (expected diameter 12:2 μm).

Figure 8c shows normalized spatial intensity profiles along one axis for increasing pumping power near the critical value. Interestingly, we observe that the mode diameter enlarges with increasing condensate fraction, as shown in figure 8d. This effect is not expected for an ideal gas of photons. In principle, this could be due to a Kerr nonlinearity in the dye solution, but the most straightforward explanation is a weak repulsive optical self-interaction from thermal lensing in the dye.

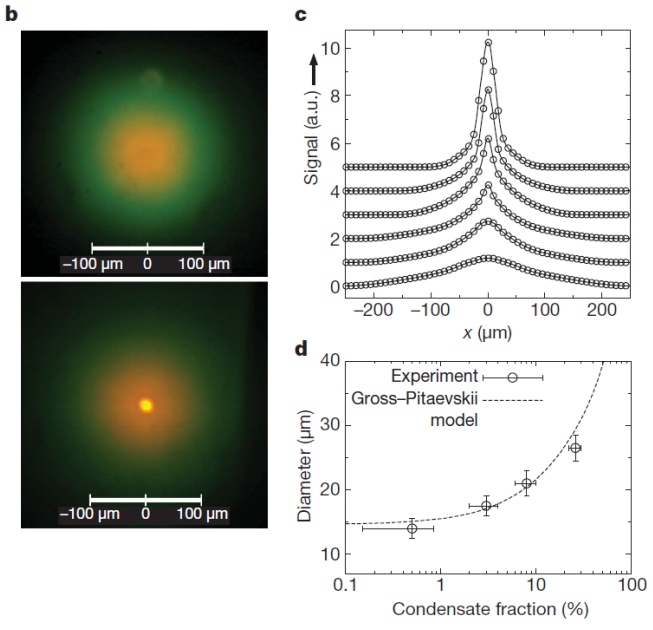

Figure 8. Images of the spatial radiation distribution transmitted through one cavity mirror both below (upper panel) and above (lower panel) criticality, showing a macroscopically occupied TEM00-mode for the latter case. c, d, Cut through the centre of the intensity distribution for increasing optical pump powers (c) and width of the condensate peak versus condensate fraction, along with a theoretical model based on the Gross–Pitaevskii equation with an interaction parameter $\tilde{g} = 7 \times 10^{-4}$.

IV. CONCLUSIONS

As a conclusion of this work, we review the concepts that lead in a general form to a quantum fluid of light, starting from optical ressonator (cavity) system in which photons are confined to be studied. Inside of this cavity is put it on a nonlinear material, generally a semiconductor, composed by a finite number of quantum wells that trap the electron in two dimension. Electrons can be excited and release from the equilibrium state an create a exciton, which is the pair particle-hole excited into the quantum well. After a while, the exciton can decay en generate a photon that can be set in resonance with the cavity. We showed that this photon can be excite another exciton, and the linear combination of the photon cavity and the exciton form a polariton. Also we saw that the photon-photon interaction is mediated by the exciton and experimentally its posible to produce superfluid of this systems. We had presented two type of experiments in which are reached the Bose-Einstein condensation for polaritons and photons.

[1] Allen, A., J.F; MISENER (1938), Nature **141** (3558), 75.
[2] Anderson, M. H., J. R. Ensher, M. R. Matthews, C. E. Wieman, and E. A. Cornell (1995), Science **269** (5221), 198, http://science.sciencemag.org/content/269/5221/198.full.pdf.
[3] Balili, R., V. Hartwell, D. Snoke, L. Pfeiffer, and K. West (2007), Science **316** (5827), 1007, http://science.sciencemag.org/content/316/5827/1007.full.pdf.
[4] Balili, R. B., D. W. Snoke, L. Pfeiffer, and K. West (2006), Appl. Phys. Lett. **88** (3), 031110.
[5] Davis, K. B., M. O. Mewes, M. R. Andrews, N. J. van Druten, D. S. Durfee, D. M. Kurn, and W. Ketterle (1995), Physical Review Letters **75** (22), 3969.
[6] KAPITZA, P. (1938), Nature **141** (3558), 74.
[7] Kasprzak, J., M. Richard, S. Kundermann, A. Baas, P. Jeambrun, J. M. J. Keeling, F. M. Marchetti, M. H. Szymanska, R. Andre, J. L. Staehli, V. Savona, P. B. Littlewood, B. Deveaud, and L. S. Dang (2006), Nature **443**, 409.